Damage-Mitigating Control With Overload Injection: Experimental Validation of the Concept[1]

Hui Zhang
Mem. ASME

Asok Ray
Fellow ASME
e-mail: axr2@psu.edu

Ravindra Patankar

Mechanical Engineering Department,
The Pennsylvania State University,
University Park, PA 16802

The goal of damage-mitigating control is to enhance structural durability of mechanical systems (e.g., advanced aircraft, spacecraft, and power plants) while retaining high performance. So far the reported work in damage-mitigating control has focused on reduction of peak stresses to increase structural durability. This paper presents a novel concept that takes advantage of the physical phenomenon of fatigue crack retardation. Overload pulses are intermittently injected into the plant as a feedforward signal through the actuator(s) in addition to robust feedback control. A feedforward sequence of limited overload pulses and a robust feedback control law are designed based on state-space models of fatigue-crack damage and plant dynamics. A series of experiments have been conducted on a laboratory test apparatus to demonstrate feasibility of the overload injection concept for robust damage-mitigating control. [S0022-0434(00)01302-2]

Keywords: Life Extending Control, Robust Control, Structural Integrity, Fatigue Crack Retardation

1 Introduction

The key idea of damage-mitigating control of mechanical structures is that substantial improvements in the service life of critical components can be achieved by insignificant reduction in the system dynamic performance (Ray et al. [1]). Further work on damage-mitigating control has been reported by Dai and Ray [2], Kallappa et al. [3], Kallappa and Ray [4], Rozak and Ray [5,6], Holmes and Ray [7], and Caplin [8] for different applications in rocket engines, fossil power plants, rotorcraft, and aircraft in the framework of both feedforward and feedback control.

Zhang and Ray [9] and Zhang et al. [10] have demonstrated the efficacy of damage-mitigating control on a laboratory test apparatus where peak stresses in a critical component are reduced to increase its structural durability. The present paper introduces a novel concept of damage-mitigating control in which a sequence of overload pulses is intermittently injected into the plant as a feedforward signal through the actuator(s) in addition to stress reduction by robust feedback control. A series of experiments have been conducted on the above laboratory test apparatus to demonstrate feasibility of the overload injection concept for damage-mitigating control. The main idea is to take advantage of the physical phenomenon of fatigue crack retardation that is briefly explained below.

While large cyclic loads of constant-amplitude are detrimental to structural durability, researchers (e.g., Schijve [11]) in the field of fracture mechanics discovered that short-duration overloads on small or medium cyclic loads of constant-amplitude could, in fact, extend the fatigue life. This claim has been experimentally validated on fatigue testing machines (e.g., McMillan and Pelloux [12]; Porter [13]; Schijve [14]). The rationale for this physical phenomenon is that an overload enlarges the plastic zone at the crack tip, which, in turn, causes compressive forces to act on the plastic zone around the crack tip region. Thus, crack growth is retarded due to an increase in the crack opening stress. Along this line, Patankar, Ray and Lakhtakia [15] and Patankar [16] have

formulated a state-space model of fatigue crack growth for damage-mitigating controller analysis and design that accounts for the impact of variable-amplitude loading on crack growth rate (e.g., crack retardation and sequence effects). Patankar and Ray [17] have also shown that the predicted structural durability (and hence the controller design) could be grossly inaccurate if the fatigue crack damage model does not capture the effects of variable-amplitude cyclic stress. In this context, the present paper shows experimental evidence of how overload injection into the control signal(s) at the actuator(s) could be beneficial for structural durability without any significant bearing on the closed loop system performance.

The paper is organized in six sections including the Introduction. Section 2 presents an overview of the state-variable-based model of fatigue crack growth and a discussion on the effects of overload on crack growth retardation. Section 3 provides a brief description of the test apparatus and an outline of experiments. Section 4 presents the design of damage-mitigating controllers with overload injection. Results of experimentation on the test apparatus are presented and discussed in Section 5. Finally, the paper is summarized and concluded in Section 6.

2 The Fatigue Crack Growth Model

Different aspects of fatigue crack damage have been reported by many investigators as cited in research monographs (e.g., Suresh [18] and Anderson [19]) on fracture mechanics. In the present paper, we have used the fatigue crack growth model of Patankar [16] in the state-space setting that has been validated with the test data of McMillan and Pelloux [12] and Porter [13] along with explanations of the underlying physical phenomena. The state-space model of fatigue crack growth is an extension of the Fastran-II model (Newman, [20,21]) which is based on the concept of small cracks in homogeneous materials. The Fastran-II model is represented by a nonlinear difference equation in which the crack increment during the kth cycle is obtained as a function of the maximum applied (far-field) stress $S_k^{\max}$ and the crack opening stress S_k^o for $k \geq 1$ and $a_0 > 0$ as:

$$\Delta a_k \equiv a_k - a_{k-1} = h(\Delta K_k^{\text{eff}}) \quad \text{with} \quad h(0) = 0$$

$$\Delta K_k^{\text{eff}} \equiv \sqrt{\pi a_{k-1}} F(a_{k-1}, w)(S_k^{\max} - S_{k-1}^o) U(S_k^{\max} - S_{k-1}^o) \tag{1}$$

where a_{k-1} and S_{k-1}^o are the crack-length and the crack-opening stress, respectively, during the kth cycle and change to a_k and S_k^o

Copyright © 2000 by ASME

Transactions of the ASME

at the expiry of the kth cycle; $F(\bullet,\bullet)$ is a crack-length-dependent correction factor compensating for finite geometry of the specimen with the width parameter w; the non-negative monotonically increasing function $h(\bullet)$ can be represented either by a closed form algebraic equation:

$$h(\Delta K_k^{\text{eff}}) = C_1 (\Delta K_k^{\text{eff}})^m \quad \text{with material constants } C_1 \text{ and } m, \tag{2}$$

or by table lookup (Newman [21]); and $U(x) = \begin{cases} 0 & \text{if } x<0 \\ 1 & \text{if } x \geqslant 0 \end{cases}$ is the Heaviside function.

We now present the structure of the difference equation that is excited by the cyclic stress input to generate the crack opening stress. To this end, we first consider the steady-state solution of the difference equation under constant amplitude load. This issue has been addressed by several investigators including Newman [22] and Ibrahim et al. [23]. The steady-state crack-opening stress S^{oss} under a constant amplitude cyclic load is a function of the minimum stress S^{min}, the maximum stress S^{max}, the constraint factor α (which is 1 for plane stress and 3 for plane strain), the specimen geometry, and the flow stress S^{flow} (which is the average of the yield strength S^y and the ultimate strength S^{ult}). These relationships are shown to be good for most ductile alloys by Newman [22]. One such empirical relation has been used in the FASTRAN-II model (Newman [21]).

The objective is to construct the difference equation for (non-negative cycle-dependent) crack opening stress S_k^o such that, under different levels of constant-amplitude load, the forcing function S_k^{oss} at the kth cycle matches the crack-opening stress derived from the following empirical relation (Newman [22]) that is valid for non-zero peak stress (i.e., $S^{\text{max}} \neq 0$):

$$S_k^{\text{oss}} = S^{\text{oss}}(S_k^{\text{max}}, S_k^{\text{min}}, \alpha_k, F)$$
$$= (A_k^0 + A_k^1 R_k + A_k^2 (R_k)^2 + A_k^3 (R_k)^3) S_k^{\text{max}} \tag{3}$$

$$\text{where} \quad R_k = \frac{S_k^{\text{min}}}{S_k^{\text{max}}} \quad \text{for all } k \geqslant 0; \tag{4}$$

$$A_k^0 = (0.825 - 0.34\alpha_k + 0.05(\alpha_k)^2)\left[\cos\left(\frac{\pi}{2}\frac{S_k^{\text{max}}}{S^{\text{flow}}}\right)\right]^{1/\alpha_k} \tag{5}$$

$$A_k^1 = (0.415 - 0.071\alpha_k)\left(\frac{S_k^{\text{max}}}{S^{\text{flow}}}\right) \tag{6}$$

$$A_k^2 = (1 - A_k^0 - A_k^1 - A_k^3)U(R_k) \tag{7}$$

$$A_k^3 = (2A_k^0 + A_k^1 - 1)U(R_k) \tag{8}$$

The constraint factor α_k used in Eqs. (5) and (6) is obtained as a function of the crack length increment Δa_k in Eq. (1). A procedure for evaluation of α_k is presented in the Fastran-II manual (Newman [21]). Since α_k does not significantly change over cycles, it can be approximated as piecewise constant for limited ranges of crack length.

The following constitutive relation in the form of a nonlinear first-order difference equation is proposed for recursive computation of the crack-opening stress S_k^o upon completion of the kth cycle (Patankar [16]):

$$S_k^o = \left(\frac{1}{1+\eta}\right)S_{k-1}^o + \left(\frac{\eta}{1+\eta}\right)S_k^{\text{oss}} + \left(\frac{1}{1+\eta}\right)(S_k^{\text{oss}} - S_{k-1}^o)$$

$$\times U(S_k^{\text{oss}} - S_{k-1}^o) + \left(\frac{1}{1+\eta}\right)[S_k^{\text{oss}} - S_k^{\text{oss\_old}}]$$

$$\times U(S_{k-1}^{\text{min}} - S_k^{\text{min}})[1 - U(S_k^{\text{oss}} - S_{k-1}^o)] \tag{9}$$

$$\eta = \frac{tS^y}{2wE} \tag{10}$$

where the forcing function S_k^{oss} in Eq. (9) is calculated from Eq. (3) as if a constant amplitude stress cycle $(S_k^{\text{max}}, S_k^{\text{min}})$ is applied; similarly, $S_k^{\text{oss\_old}}$ is given by Eq. (3) as if a constant amplitude stress cycle $(S_k^{\text{max}}, S_{k-1}^{\text{min}})$ is applied. For constant-amplitude loading, S^{oss} is the steady-state solution of S_k^o. In general, the inputs S_k^{oss} and $S_k^{\text{oss\_old}}$ to Eq. (9) are different from the instantaneous crack-opening stress S_k^o under variable-amplitude loading. The Heaviside function $U(S_k^{\text{oss}} - S_{k-1}^o)$ in the third term on the right-hand side of Eq. (9) allows fast rise and slow decay of S_k^o. The last term on the right-hand side of Eq. (9) accounts for the effects of reverse plastic flow. Depletion of the normal plastic zone occurs when the minimum stress S_k^{min} decreases below its value S_{k-1}^{min} in the previous cycle, which is incorporated via the Heaviside function $U(S_{k-1}^{\text{min}} - S_k^{\text{min}})$. Note that the overload excitation and reverse plastic flow are mutually exclusive.

The dimensionless parameter η in Eq. (10) depends on the component thickness t, half-width w, yield strength S^y, and Young's modulus E. Alternatively, Eq. (10) could be used to generate an estimate of η that can be fine-tuned by parameter identification using available test data. Following an overload cycle, the duration of crack retardation is controlled by the transients of S_k^o in the state-space model, and hence determined by the stress-independent parameter η in Eqs. (9) and (10). Physically, this duration depends on the ductility of the material that is dependent on many factors including the heat treatment of specimens (Schijve [14]). Smaller yield strength produces a smaller value of η, resulting in longer duration of the overload effect. Smaller specimen thickness has a similar effect (Schijve [14]). Equations (1)–(10) describe the state-space model where the crack length a_k and crack opening stress S_k^o are the state variables.

The net effect of a single-cycle overload (i.e., increased S_k^{max}) is a jump in the effective stress range $\Delta S_k \equiv S_k^{\text{max}} - S_k^o$ resulting in an increase in the crack growth increment in the present cycle. Shortly after the expiration of the overload (i.e., S_k^{max} returning to the original lower value), S_k^o starts decreasing slowly from its increased value. The result is a decrease in ΔS_k, which causes the crack growth rate to diminish. Subsequently, after returning to the original constant-amplitude stress, as S_k^o slowly relaxes back to its original state, the crack growth rate resumes the original value. A single overload initially increases crack growth rate for a few cycles and then gradually decreases over a much higher number of cycles until it reaches the original value. The crack growth is therefore retarded due to the fast rise and slow decay of S_k^o.

The control system, presented later in Section 4, requires injection of a sequence of overload pulses. The interval (i.e., the spacing between the consecutive overload injections) and the magnitude of the injected overload pulses that influence the crack growth rate must be appropriately designed to achieve the beneficial effects of crack retardation in damage-mitigating control. Both interval and magnitude of overload injection are critical for damage-mitigating control systems design. The interval of overload injection could be largely determined from the transients of the crack opening stress S_k^o. For example, if S_{k-1}^o is close to S_k^{max}, fatigue damage in the stress cycle is insignificant due to small ΔS_k, and consequently, there is no appreciable benefit from overload injection. Similarly, the magnitude of overload injection could be dominated by the current state of crack length a_k. It is natural to inject a small overload (or no overload) if the current state a_k is relatively large for which the immediate penalty might be unacceptably large. In the extreme case, immediate failure may occur due to a large overload.

3 The Test Apparatus

The test apparatus is briefly described in this section. Zhang and Ray [9] have reported the details of mechanical design and

instrumentation of the test apparatus including the dominant modes of vibration. The test apparatus is designed and fabricated as a three-degree-of-freedom (DOF) mass-beam structure excited by the oscillatory motion of two vibrators as shown in Fig. 1 and the dimensions of the pertinent components are listed in Table 1. Two out of the three DOFs are directly controlled by the two actuators (i.e., Vibrator#1 and Vibrator#2) and the remaining DOF is observable via displacement measurements of the three vibrating masses: Mass#1, Mass#2, and Mass#3. The inputs to the multivariable mechanical structure are the forces exerted by the two actuators; the output to be controlled is the displacement of Mass#1. A failure site is introduced as a circular hole of radius 3.81 mm centered at a distance of 25.4 mm from Mass#3 in the test specimen (Beam#2) which represents a critical plant component subjected to fatigue crack damage.

The test apparatus is logically partitioned into two subsystems: (i) the plant subsystem consisting of the mechanical structure including the test specimen to undergo fatigue damage, actuators, and sensors; and (ii) the control and instrumentation subsystem consisting of computers, data acquisition and processing, and communications hardware & software. The frequency of the (square-wave) reference signal is 2.07 Hz that is one third of the first modal frequency ($\sim$6.21 Hz) of the test apparatus structure. Hence, the third harmonic of the reference signal excites the structure at the resonance frequency of 6.21 Hz. Thus, the test specimen can be excited at different levels of cyclic stress via vibratory motion of Mass#3 with no significant change in the external power injection into the actuators.

The material of the test specimen is 6063-T6 aluminum alloy. The model parameters in Eqs. (1)–(10) are evaluated from the estimated mean of fatigue life based on an ensemble of experiments conducted on the test apparatus. Since the model of geometry factor F in Eq. (1) under bending stress is not readily available in the literature, it is assumed to be structurally similar to that for center-cracked specimens under uniaxial tension, i.e., F
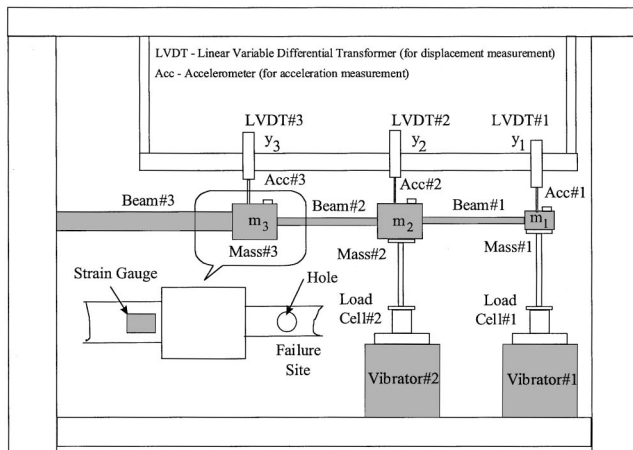
$= \sqrt{s(\pi a/2w)}$ where $w = 5.55$ mm is the half-width of the test specimen. The initial crack length is set as the radius of the hole on Beam#2, i.e., $a_0 = 3.81$ mm in Eq. (1). Table 2 and Table 3 list the material parameters of 6063-T6 (Kumar [24]) and the experimentally evaluated model parameters of the fatigue crack growth Eqs. (2) and (10), respectively. The cyclic stress at the failure site is the damage-causing variable that needs to be appropriately regulated by the damage-mitigating controller for enhancement of structural durability without any significant loss of the system performance. The far-field cyclic stress $S^{\mathrm{nom}}(t)$ at the free surface of the failure site is obtained from a finite-element model of the test apparatus structure and is validated with experimental data of strain measurements to be within five percent accuracy. This model generates $S^{\mathrm{nom}}(t)$ in real time as an algebraic function of the displacement measurements of the three vibrating masses: Mass#1, Mass#2, and Mass#3:

$$S^{\mathrm{nom}}(t) = \sum_{k=1}^{3} \beta_k y_k(t) \quad \text{with} \quad \beta_1 = 1.5025; \beta_2 = -9.4095;$$

$$\beta_3 = 13.1437 \text{ in SI units} \tag{11}$$

4 The Damage-Mitigating Control System With Overload Injection

We define the tracking ability of Mass#1 in Fig. 1 to follow the square wave reference signal as a performance requirement for damage-mitigating control (DMC). A robust controller is designed following a conventional setup consisting of a generalized plant model that is derived with additional consideration of fatigue damage for structural durability. In Fig. 2, $G_{\mathrm{nom}}(s)$ is the nominal plant model of the test apparatus and $W_{\mathrm{del}}(s)$ is the model of additive frequency-dependent uncertainties. Both $G_{\mathrm{nom}}(s)$ and $W_{\mathrm{del}}(s)$ have been generated from experimental data using a frequency-domain identification procedure (Zhang and Ray [9]). The frequency-dependent performance weighting matrix $W_p(s)$ penalizes the tracking error, e, of Mass#1 displacement to achieve a trade-off between performance and stability robustness. Synthesis of the damage-mitigating control law makes use of two additional weighting matrices:

- $W_{pd}(s)$ to penalize the displacement y_3 of Mass#3 that strongly influences the damage-causing variable S^{nom} in Eq. (11); and
- $W_{\mathrm{cont}}(s)$ to penalize the amplitude of the damage-causing frequency (i.e., the resonance frequency of $\sim$6.21 Hz) component in the control action.

Fig. 1 Schematic diagram of the test apparatus

Table 1 Structural dimensions of the test apparatus

Component	Material	Dimensions (mm) length× width× thickness
Mass #1	Mild Steel	101.6× 76.2× 38.1
Mass #2	Aluminum 6063-T6	101.6× 76.2× 25.4
Mass #3	Aluminum 6063-T6	63.5× 38.1× 50.8
Beam #1	Mild Steel	711.2× 21.3× 11.1
Beam #2	Aluminum 6063-T6	355.6× 11.1× 3.1
Beam #3	Mild Steel	457.2× 19.1× 6.4

Total length of the test apparatus structure = 1,790.7 mm
Diameter of the hole in Beam#2 = 7.62 mm

Table 2 Properties of 6063-T6 aluminum alloy

Material Parameter	Value
Yield stress S^y	201 MPa
Ultimate Stress S^{ult}	230 MPa
Young's modulus E	72×10^3 MPa
Strain Hardening Exponent	0.06
Reduction in Area	57.12%
Elongation	15.84%

Table 3 Experimentally evaluated model parameters

Model Parameter	Value
C_1 in Eq. (2)	0.62×10^{-12} (SI Units)
m in Eq. (2)	3.8 (dimensionless)
α in Eqs. (5) and (6)	1.6 (dimensionless)
η in Eq. (9)	0.8×10^{-3} (dimensionless)

A robust control law $K_{DMC}(s)$ is formulated by optimization of the overall system performance in the following form (Zhou et al. [25]):

$$k_{DMC}^{min}\{\|F_u(F_l(P_{DMC}(s),K_{DMC}(s)),\Delta(s))\|_\infty$$

$$< 1 \;\; \forall \Delta(s) \quad \text{with} \;\; \|\Delta(s)\|_\infty \leqslant 1\} \qquad (12)$$

where $F_u(\cdot,\cdot)$, $F_l(\cdot,\cdot)$, and $\Delta(s)$ are upper and lower Linear Fractional Transform (LFT) operators, respectively; $\Delta(s)$ is the block structure of modeling uncertainty represented by a matrix of compatible dimension; and $P_{DMC}(s)$ is the generalized plant model obtained by augmenting the nominal plant model $G_{nom}(s)$ with the uncertainty weight $W_{del}(s)$ and the performance weights $W_p(s)$, $W_{pd}(s)$, and $W_{cont}(s)$ following Fig. 2. The H_∞-optimal cost functional guarantees exact loop-shaping relative to the preset weighting functions W_{del} and W_p, thereby achieving uncertainty tolerance and disturbance rejection. The models of nominal plant dynamics, and (frequency-dependent) uncertainty and performance weights are presented in a previous publication (Zhang and Ray [9]).

Theme of Damage-Mitigating Control With Overload Injection. The objective here is to introduce and experimentally validate the concept of overload (i.e., intermittent large peak stress) injection as an augmentation of the existing concept of damage-mitigating control (Zhang and Ray [9]; Holmes and Ray [7]) that reduces instantaneous peak stresses by penalizing the damage-causing variable(s) in the H_∞ setting. The concept of peak stress reduction at the critical component(s) is retained in the present control philosophy because it acts as a deterrent against large fatigue damage that might result from exogenous disturbances. Removal of this penalization in the control synthesis procedure would defeat the purpose of damage mitigating control as the structural durability of the plant might be endangered due to excessive peak stresses. On the other hand, solely relying on peak stress reduction may not take advantage of the physical phenomenon of crack retardation for enhancement of structural durability especially under transient operations (Patankar and Ray [17]). The theme of damage-mitigating control with overload injection is briefly explained below in the context of experimental validation on the test apparatus.

A sequence of overload pulses is injected into Vibrator#2 of the test apparatus (see Fig. 1). This sequence of pulses serves as a feedforward input that is additively superimposed on the feedback control signal as seen in Fig. 2. The key idea is that the feedback controller attempts to maintain the stress amplitude at a safe level for a relatively long period while the intermittently injected overload pulses produce the desired beneficial effects of crack retardation. The robust feedback controller views the feedforward signal as an exogenous input and consequently attempts to compensate the effects of the overload pulses as disturbance re-

jection. This leads to mitigation of the long-term effects of the injected overload pulses, which is highly advantageous in the sense that a single-cycle overload injection is most beneficial for crack retardation (Schijve [14]; Patankar et al. [15]). The disturbance rejection property of the robust controller thus becomes very important for reduction of the undesirable long-term effects of the injected overload sequence to retain the specified performance upon overload injection. In essence, the feedforward signal attempts to provide the beneficial effects of crack retardation, and the feedback controller yields robust performance via disturbance rejection. The experiments on the test apparatus investigate whether the interactions of these two control signals enhance the objective of damage-mitigating control, i.e., achieving structural durability with no significant loss of dynamic performance. The anticipated results are an increase the fatigue life of the test specimen with no appreciable change in performance (i.e., the displacement profile of Mass#1 in Fig. 1).

Remark 1: The control problem at hand is different from that on a standard fatigue testing machine, in which an actuator directly applies an overload pulse to a test specimen in one cycle and the original load cycle is resumed in the subsequent cycles. In contrast, an overload signal can only be indirectly applied to critical components of mechanical systems such as an aircraft. It may take a longer period of time to alter the stress profile at the failure site. In essence, the actuator and plant dynamics serve as a (fading-memory) low-pass filter that spreads the effects of the injected overload pulse for a longer duration. Therefore, a combination of feedforward and robust feedback control is necessary to realize the concept of damage-mitigating control with overload injection in complex mechanical systems. The major objective of damage-mitigating control is to achieve either the specified dynamic performance with minimum structural degradation, or maximum dynamic performance without exceeding the specified structural degradation. In either case, the control system must focus on dynamic performance.

Remark 2: The crack retardation effects have been observed on fatigue testing machines by superimposing short-time static overload on constant-amplitude cyclic load (Porter [13]; Schjive [14]) where the sole purpose is destructive evaluation of specimen life. The purpose of damage-mitigating control is different. Dynamic performance of a damage-mitigating control system could be significantly degraded by injection of such a static overload at an arbitrary instant. The instant of overload injection is critical for retaining the high dynamic performance while achieving increased fatigue life of structural components. Therefore, the dynamics of the closed loop control system must determine the instant of overload injection as a feedforward signal. A possible configuration of damage-mitigating control is a hierarchical structure (Holmes and Ray [7]) where a supervisory controller in the upper tier generates the feedforward signal of overload injection into the robust feedback controller in the lower tier. It should be noted that limitations on operating procedure, safety requirements, and actuator saturation may not often allow much freedom for variations in the amplitude of injected overload pulses in operating machinery. To this end, experiments presented in Section 5 are designed for a constant value of overload amplitude injected at different intervals.

Generation of Overload Pulse Sequences. Timely injection of overload pulses is critical for retention of the control system performance as discussed above. For example, in the experiments on the test apparatus, an overload pulse must increase the peak value of the stress cycle in the specimen, whose magnitude and the instant of occurrence must be accurately determined. An inspection of the mode shapes (Zhang and Ray [9]) of the test apparatus structure reveals that the point of maximum bending stress corresponds to the instant when the displacement of Mass#3 in Fig. 1 is at its peak. The controller must be able to identify these instants in the discrete-time domain, at least one sampling interval prior to injection of the overload. This information is then used to
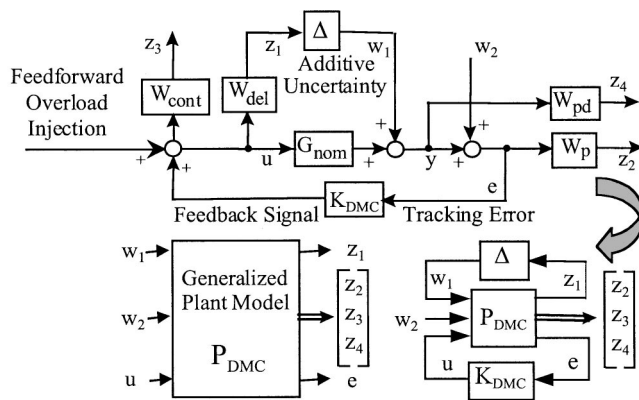

Fig. 2 Linear robust control system

inject the overload pulse as the state of maximum stress occurs next.

In order to introduce the overload, one can either increase the displacement of Mass#3 or reduce the displacement of Mass#2. Either or both actions increase the maximum bending stress on the specimen. Since the position of Mass#3 is not directly controlled by any one of the two actuators, the overload is introduced through Vibrator#2 that directly acts upon Mass#2. It follows from Eqs. (1) and (9) that injection of a negative displacement pulse on Mass#2 increases the bending stress on the specimen leading to the overload effect. The desired magnitude of the overload pulse is injected as a feedforward signal to Vibrator#2 without exceeding its physical restrictions (e.g., electrical and mechanical constraints of the actuator). The strategy of overload injection on the test apparatus is summarized below.

The controller detects the point of maximum relative displacement between Mass#2 and Mass#3, one sampling period prior to the application of the overload. This instant in the discrete-time domain corresponds to the maximum of the cyclic stress in the specimen. The above information is used to inject the overload by applying a negative pulse as a feedforward signal to Vibrator#2. Since an overload injection is an exogenous disturbance to the robust feedback control system, it generates an input sequence to Vibrator#1 so that the combined effects of this feedback control signal and the injected overload would satisfy the performance requirement. In other words, the overload injection should not have any significant influence on the system performance, i.e., the displacement profile of Mass#1.

Implementation of the Control System on the Test Apparatus. The feedback control system and overload sequences are implemented on a Pentium PC along with necessary A/D and D/A interface to the amplifiers serving the sensors and actuators of the test apparatus. Overload signals are superimposed on the feedback control signal at Vibrator#2 at the required interval as discussed earlier in Section 2. Control signals are passed down to the two power-amplifier-driven vibrators and three linear variable differential transformers (LVDTs) measure the displacements of the three masses. The displacement of Mass#1 is the feedback signal to the performance controller while the stress $S^{nom}(t)$ is calculated on-line as a linear combination of the displacements of all three masses as defined in Eq. (11). This information is transmitted over the network to another computer where the crack length and crack growth rate are simultaneously computed. At present, the information on stress transients is used for off-line generation of the overload sequence. In the follow-up research, a supervisory controller will be designed for generation of overload sequences in real time by using the information on stress transients.

5 Experimental Results and Discussion

This section presents the experimental results describing the effects of overload injection on the plant performance and structural durability, i.e., life of test specimens. Figure 3 shows displacements of the three masses in the test apparatus as well as the input signals to the two vibrators. For a constant-amplitude load, the motion of Mass#3 corresponds to the natural frequency ($\sim$6.21 Hz) of the test apparatus structure undergoing three oscillations for each period of motion of Mass#1 and Mass#2 as depicted in the top plate of Fig. 3. Mass#1 closely follows the reference signal of square-wave motion (at 2.07 Hz) with and without overload injection. As stated earlier, the main objective of damage-mitigating control is to enhance structural durability with no significant loss of performance. Therefore, the proposed concept of damage mitigation must ensure disturbance rejection with the goal of having the displacement profile of Mass#1 unaffected by the overload injection. The constant amplitude of the stress cycles at the failure site is interrupted by the overload induced through the application of a disturbance signal at Vibrator#2. The

injected disturbance is seen in the bottom plate of Fig. 3 as a negative signal that reduces the displacement of Vibrator#2 thus causing Mass#2 to move downwards. At the same time, Mass#3 moves upward and is at its highest position thus causing the maximum bending stress on the specimen and hence the overload is applied at this instant.

The plots in the top plate of Fig. 3 depict the effects of overload on the control system performance. The sequence of overload signals is injected as an input to Vibrator#2 that is directly coupled to Mass#2 (see Fig. 1) and hence its impact on its position is prominent as seen in Fig. 3. The effects of overload are also significant from the point of view of stress at the crack site located on the test specimen that couples Mass#2 and Mass#3. In contrast, due to the disturbance rejection feature of the control system, the effects of the overload are insignificant from the perspectives of performance requirement, i.e., the motion of Mass#1 is practically unaffected by the overload injection as seen in the top plate of Fig. 3. This is explained as follows. The control system detects the disturbance injected through Vibrator#2 from the sensor signal of Mass#2 displacement. In the subsequent samples, the controller makes appropriate adjustments in the input sequence to Vibrator#1 as seen in the bottom plate of Fig. 3. The combined effects of the overload injection and the altered feedback control inputs to Vibrator#1 allows Mass#1 to closely follow the specified trajectory. In other words, the robust feedback controller filters the effects of the injected overload pulse in such a way that the performance (i.e., the displacement profile of Mass#1) is practically unaffected. The filtering action causes small changes in the control signal to Vibrator#1 as seen in the bottom part of Fig. 3.

The effects of overload injection on the specimen life have been investigated under five different loading conditions with six specimens for each. The estimated mean of fatigue life is listed in Table 4 and the estimated standard deviation for each load is found to be about 6000 cycles. The first condition is a constant-amplitude load excitation (i.e., with no overload injection) with $S^{max}=47$ MPa and $S^{min}=11.2$ MPa of the nominal cyclic stress $S^{nom}(t)$ obtained as a function of the displacement measurements in Eq. (11). These values of S^{max} and S^{min} serve as a benchmark for evaluation of the specimen life under the remaining four conditions of overload injection. The disturbance injected at Vibrator#2 superimposes an overload-underload pulse on the constant amplitude load sequence to yield transient peak stresses of $S^{max}=54$ MPa and $S^{min}=9.8$ MPa. These pulses are injected at constant intervals and the interval periods are different for the three overload conditions listed in Table 4. Introducing the overload sequence at an interval of 5100 cycles increases the specimen life, calculated as an ensemble average of six test data points, from 36,667 cycles to 47,700 cycles (i.e., an increase by $\sim$30 percent). Upon decreasing the overload injection interval from 5100 cycles
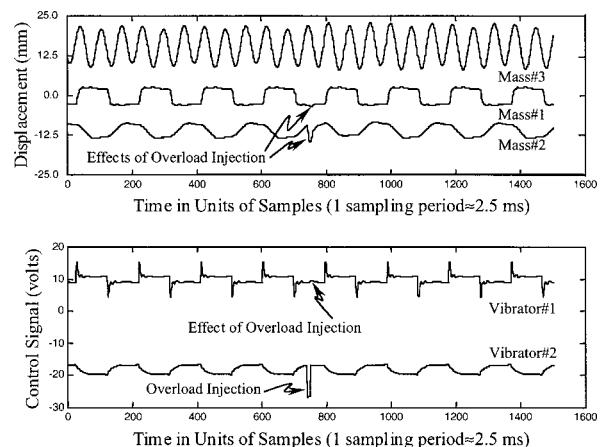

Fig. 3 Impact of overload injection on system performance

Table 4 Estimated mean of fatigue life under overload injection

Description of Experiments	Average Specimen Life (cycles)	Model Prediction (cycles)
Base load: $\begin{cases} S^{max} = 47.0\,\text{MPa} \\ S^{min} = 11.2\,\text{MPa} \end{cases}$		
No Overload	36,667	35,000
Overload/Underload: 54 Mpa/9.8 MPa @ 5,100 cycles	47,700	46,000
Overload/Underload: 54 MPa/9.8 MPa @ 2,400 cycles	49,200	50,000
Overload/ Underload: 54 MPa/9.8 MPa @ 900 cycles	54,543	54,000
Overload/Underload: 54 MPa/9.8 MPa @ 0 cycles	25,200	25,875

\# of test samples in each case = 6
Estimated standard deviation in each case = ~6,000 cycles

to 2400 cycles, the average specimen life is found to increase to 49,200 cycles (i.e., by an additional ~5 percent). A further decrease in the overload interval from 2400 cycles to 900 cycles, the average specimen life is found to increase to 54,543 cycles, which is an overall increase of ~50 percent over the case without any overload injection. Although a gradual decrease from 900 cycles did not conclusively increase the average specimen life, a significant decrease of the overload interval close to zero cycles showed a reverse trend of decreasing average specimen life. A precise value of the overload interval (between 0 and 900 cycles) at which the average specimen life is maximized could not be established from these experiments and therefore is not reported.

The above observations support the hypothesis of the concept reported in this paper—the injection of a stress overload can increase the fatigue life of a critical plant component. Furthermore, as discussed earlier, the robust control system can be designed such that the injected overload sequence has no significant influence on the dynamic performance and hence the concept of damage-mitigating control with overload injection becomes feasible. However, since there is a penalty of instantaneous crack increment associated with each overload, further reduction of the interval beyond a certain point will no longer increase the fatigue life. For example, with a short interval between consecutive overloads, the gain in life due to crack retardation may not be able to compensate for the larger instantaneous crack growth induced by the overload itself. Because of the cumulative penalty associated with a large number of overloads, the specimen life will actually decrease with very frequent injection of overload. The extreme case of zero overload interval, i.e., application of overload at every cycle, is equivalent to having a constant-amplitude load with $S^{max} = 54$ MPa and $S^{min} = 9.8$ MPa. The fatigue life is reduced to 25,200 cycles as compared with 36,667 cycles under the original constant-amplitude load with $S^{max} = 47$ MPa and $S^{min} = 11.2$ MPa (see Table 4). Therefore, excessive reduction of the overload interval will cause premature damage compared to constant-amplitude loading with no overload injection.

The last column in Table 4 lists the model prediction of fatigue life (i.e., the number of cycles to break the specimen) for the constant-amplitude base load, the three cases of overload injection, and the constant-amplitude overload. Equations (1)–(10) are numerically solved for initial crack length $a_0 = 4.76$ mm (radius of the hole on Beam#2) and with (far-field) stress data $S^{nom}(t)$ at the failure site as the input. The model predictions are in close agreement with the experimental data of estimated mean of fatigue life.

Remark 3: The results in Table 4 are presented for a single operating point in terms of fixed S^{max} and S^{min}. Limitations of the test apparatus, due to actuator saturation and bandwidth, may not permit experimentation with higher stress amplitudes representing

low-cycle fatigue. Although the test apparatus allows smaller stress amplitudes representing high-cycle fatigue, the experimentation time needed to break a specimen is relatively much larger. Considering wear and tear of the test apparatus, only very few such experiments were conducted and the savings in fatigue life were found to be significantly higher due to relatively larger amount of allowable injected overload. These results are not presented in this paper due to insufficiency of data.

6 Summary and Conclusions

The goal of damage-mitigating control is to achieve high performance with increased reliability, availability, component durability, and maintainability in complex mechanical systems such as advanced aircraft, spacecraft, and power plants. So far the reported work in damage-mitigating control has focused on reduction of peak stresses to increase structural durability. This paper presents experimental validation of a novel concept of robust damage-mitigating control with feedforward injection of overload pulses. The feedback controller is designed based on the H_∞-approach with due consideration to robust performance. Different overload sequences are generated based on state-space models of damage and plant dynamics.

Experiments have been conducted on a test apparatus that is a three degree-of-freedom vibrating structure equipped with computer control and instrumentation. Results demonstrate that fatigue life of test specimens can be substantially extended with no noticeable degradation in the dynamic performance of the mechanical system by injecting overload at certain specified intervals in addition to feedback control. The important conclusion drawn from these experiments is that damage-mitigating control with overload injection is potentially capable of yielding substantial increase in structural durability of machinery components without compromising the dynamic performance. However, since there is a penalty of instantaneous crack increment associated with each overload, reduction of the overload interval beyond a certain range no longer increases the fatigue life. Because of the cumulative penalty associated with a large number of overloads, the fatigue life actually decreases with very frequent injection of overload.

Full benefits of overload injection can be derived by varying the interval and magnitude of injected overload pulses based on the plant operating condition, damage states, and mission objectives. This would require real-time information fusion of the plant dynamics and sensor data with the knowledge of damage states and prescribed service life. A possible configuration of damage-mitigating control is a hierarchical structure where a supervisory controller in the upper tier generates the feedforward signals of overload injection into the robust feedback controller in the lower tier. This is a subject of current research.

The results generated in this paper convey a clear message that damage-mitigating control with overload injection could have a considerable beneficial effect for life extension of critical components of mechanical systems. If one is willing to pay the price of additional instrumentation and (possibly) small loss of performance, there is a strong potential for much larger gains in structural durability. Controller design with overload injection requires a careful study of material properties. Specifically, it should be recognized that the physics of fatigue damage in a laboratory test apparatus is, in most cases, significantly different from that at actual operating environment of a plant. Extensive analytical and experimental research is necessary before implementation of damage-mitigating control with overload injection in an operating plant.

References

[1] Ray, A., Wu, M.-K., Carpino, M., and Lorenzo, C. F., 1994, ''Damage-Mitigating Control of Mechanical Systems: Parts I and II,'' ASME J. Dyn. Syst., Meas., Control, **116**, No. 3, pp. 437–455.

[2] Dai, X., and Ray, A., 1996, ''Damage-Mitigating Control of a Reusable Rocket Engine: Parts I and II,'' ASME J. Dyn. Syst., Meas., Control, **118**, No. 3, pp. 401–415.

[3] Kallappa, P., Holmes, M., and Ray, A., 1997, ''Life Extending Control of Fossil Power Plants for Structural Durability and High Performance,'' Automatica, **33**, No. 6, pp. 1101–1118.

[4] Kallappa, P., and Ray, A., 2000, ''Fuzzy Wide-Range Control of Fossil Power Plants for Life Extension and Robust Performance,'' Automatica, **36**, No. 1, pp. 69–82.

[5] Rozak, J. N., and Ray, A., 1997, ''Robust Multivariable Control of Rotorcraft in Forward Flight,'' J. Am. Helicopter Soc., **42**, No. 2, pp. 149–160.

[6] Rozak, J. N., and Ray, A., 1998, ''Robust Multivariable Control of Rotorcraft in Forward Flight: Impact of Bandwidth on Fatigue Life,'' J. Am. Helicopter Soc., **43**, No. 3, pp. 195–201.

[7] Holmes, M. S., and Ray, A., 1998, ''Fuzzy Damage Mitigating Control of Mechanical Structures,'' ASME J. Dyn. Syst., Meas., Control, **120**, No. 2, pp. 249–256.

[8] Caplin, J., 1998, ''Damage-Mitigating Control of Aircraft for High Performance and Life Extension,'' Ph.D. dissertation, Department of Mechanical Engineering, The Pennsylvania State University, University Park, PA.

[9] Zhang, H., and Ray, A., 1999, ''Robust Damage Damage-Mitigating Control of Mechanical Structures: Experimental Validation on a Test Apparatus,'' ASME J. Dyn. Syst., Meas., Control, **117**, No. 3, pp. 377–385.

[10] Zhang, H., Ray, A., and Phoha, S., 2000, ''Hybrid Life Extending Control of Mechanical Systems: Experimental Validation of the Concept,'' Automatica, **36**, No. 1, pp. 23–36.

[11] Schijve, J., 1961, ''Fatigue Crack Propagation in Light Alloy Sheet Material and Structure,'' *Advances in Aeronautical Sciences*, 3, Pergamon Press, p. 387.

[12] McMillan, J. C., and Pelloux, R. M. N., 1967, ''Fatigue Crack Propagation Under Program and Random Loads,'' Fatigue Crack Propagation, ASTM STP 415, pp. 505–532 (also BSRL Document D1-82-0558, 1966).

[13] Porter, T. R., 1972, ''Method of Analysis and Prediction for Variable Amplitude Fatigue Crack Growth,'' Eng. Fract. Mech., **4**, pp. 717–736.

[14] Schijve, J., 1976, ''Observations on the Prediction of Fatigue Crack Growth Propagation under Variable-Amplitude Loading,'' Fatigue Crack Growth under Spectrum Loads, ASTM STP 595, pp. 3–23.

[15] Patankar, R., Ray, A., and Lakhtakia, A., 1998, ''A State-Space Model of Fatigue Crack Dynamics,'' Int. J. Fract., **90**, No. 3, pp. 235–249.

[16] Patankar, R., 1999, ''Modeling Fatigue Crack Growth for Life-Extending Control,'' Ph.D. dissertation, Department of Mechanical Engineering, The Pennsylvania State University, University Park, PA.

[17] Patankar, R., and Ray, A., 1999, ''Damage Mitigating Controller Design for Structural Durability,'' IEEE Trans. Control Syst. Technol., **7**, No. 5, pp. 606–612.

[18] Suresh, S., 1991, *Fatigue of Materials,* Cambridge University Press, Cambridge, UK.

[19] Anderson, T. L., 1995, *Fracture Mechanics Fundamentals and Applications*, CRC Press, Inc., Boca Raton, FL.

[20] Newman, Jr., J. C., 1981, ''A Crack-Closure Model for Predicting Fatigue Crack Growth under Aircraft Loading,'' Methods and Models for Predicting Fatigue Crack Growth under Random Loading, ASTM STP 748, pp. 53–84.

[21] Newman, Jr., J. C., 1992, ''FASTRAN-II—A Fatigue Crack Growth Structural Analysis Program,'' *NASA Technical Memorandum 104159*, Langley Research Center.

[22] Newman, Jr., J. C., 1984, ''A Crack Opening Stress Equation for Fatigue Crack Growth,'' Int. J. Fract., **24**, pp. R131–R135.

[23] Ibrahim, F. K., Thompson, J. C., and Topper, T. H., 1986, ''A Study of Effect of Mechanical Variables on Fatigue Crack Closure and Propagation,'' Int. J. Fatigue, **8**, No. 3, pp. 135–142.

[24] Kumar, R., 1990, ''Experimental Observation of Crack Propagation in 6063-T6 Al-Alloy Under Constant Amplitude Loading,'' Int. J. Pressure Vessels Piping, **42**, pp. 303–315.

[25] Zhou, K., Doyle, J. C., and Glover, K., 1996, *Robust and Optimal Control*, Prentice-Hall, New Jersey.